cmgh
CELLULAR AND MOLECULAR GASTROENTEROLOGY AND HEPATOLOGY

ORIGINAL RESEARCH

A Novel Role for Kruppel-like Factor 14 (KLF14) in T-Regulatory Cell Differentiation

Olga F. Sarmento,[1] Phyllis A. Svingen,[1] Yuning Xiong,[1] Ramnik J. Xavier,[2] Dermot McGovern,[3] Thomas C. Smyrk,[4] Konstantinos A. Papadakis,[1] Raul A. Urrutia,[1] and William A. Faubion[1]

[1]*Epigenetics and Chromatin Dynamics Laboratory, Division of Gastroenterology and Hepatology and Translational Epigenomic Program, Center for Individualized Medicine, Mayo Clinic, Rochester, Minnesota;* [2]*Massachusetts General Hospital, Harvard Medical School, Boston, Massachusetts;* [3]*Cedars Sinai Hospital, Los Angeles, California;* [4]*Laboratory and Medical Pathology, Mayo Clinic, Rochester, Minnesota*

SUMMARY

KLF14 represses FOXP3 expression through an epigenetic mechanism involving the recruitment of the HP1 family of chromatin-modifying complexes to the promoter locus. The lack of KLF14 results in the differentiation of peripheral/induced T-regulatory cells and protection from colitis.

BACKGROUND & AIMS: Kruppel-like Factor 14 (KLF14) proteins function as epigenetic reprogramming factors during cell differentiation in many cell populations and in engineered induced pluripotent stem cells. In this study, we determined the function of KLF14 in the regulation of forkhead box protein 3 (FOXP3), a transcription factor critical for T regulatory (Treg) cell differentiation.

METHODS: We studied the effects of KLF14 on FOXP3 expression at the level of the protein and mRNA. We evaluated the functional relevance of KLF14 to FOXP3$^+$ Treg cells in vitro and in vivo through suppression assays and two colitis models. Finally, we analyzed the effect of KLF14 on the epigenetic landscape of the FOXP3 promoter locus through chromatin immunoprecipitation (ChIP) assay.

RESULTS: KLF14, induced upon activation of naïve CD4$^+$ T cells, segregates to the FOXP3$^-$ population and is inversely associated with FOXP3 expression and Treg function. KLF14 knockout (KO) CD4$^+$ cells differentiated into adaptive Tregs more readily in vitro and in vivo. KLF14 KO cells demonstrated an enhanced Treg suppressor function in vitro and in vivo. KLF14 repressed FOXP3 at the level of the mRNA and protein, and by ChIP assay KLF14 was found to bind to the Treg-specific demethylation region (TSDR) enhancer region of FOXP3. Furthermore, loss of KLF14 reduced the levels of H3K9me3, HP1, and Suv39H1at the TSDR.

CONCLUSIONS: These results outline a novel mechanism by which KLF14 regulates Treg cell differentiation via chromatin remodeling at the FOXP3 TSDR. To our knowledge, this is the first evidence to support a role for KLF14 in maintaining the differentiated state of Treg cells, with an outline of a potential mechanism to modify the expression of immune genes such as FOXP3 that are critical to T-cell fate. *(Cell Mol Gastroenterol Hepatol 2015;1:188–202; http://dx.doi.org/10.1016/j.jcmgh.2014.12.007)*

Keywords: FOXP3; H3K9Me3; KLF14; T-regulatory cell; TSDR.

Our laboratory focuses on the role of the evolutionarily conserved family of Kruppel-like factor (KLF) proteins in the differentiation of immune cells,[1,2] This important family of transcription factors is composed of 17 members characterized by the presence of their conserved DNA-binding domain. This domain features three Cys2/His2 zinc-fingers similar to Sp1 at the carboxyl terminus. The C-terminal zinc-fingers recognize and bind to the GT/GC-rich cis-regulatory sites found in gene promoters and enhancers. Members of the KLF family share a nuclear localization signal sequence and a transcriptional regulatory domain localized in their N-terminal portion. This N-terminus is highly variable and confers functional specificity to KLF interactions with distinct nuclear proteins. This interaction leads to gene activation, gene repression, or both.

KLF proteins have elicited significant attention due to their potential use in nuclear reprogramming, a role that leads to the acquisition and maintenance of differentiated phenotypes in induced pluripotent stem cells. This important feature of KLF proteins provides the medical community with unique tools for generating differentiated cells for use in regenerative medicine. Thus, we are optimistic that significant effort devoted to the study of KLF proteins in the immune system will increase our understanding of normal immunology, immunopathology, and immune cell therapy.

Previously, we identified a critical role for KLF10 in the epigenetic regulation of the core promoter locus of forkhead box protein 3 (FOXP3),[1] KLF10 deficiency resulted in impaired T-regulatory cell (Treg) differentiation and

Abbreviations used in this paper: **CAR, Coxsackie adenovirus receptor; ChIP, chromatin immunoprecipitation; DSS, dextran sodium sulfate; FOXP3, forkhead box protein 3; KLF, Kruppel-like factor; KO, knockout; PCR, polymerase chain reaction; RAG, recombinase activating gene-1-deficient; S1P1, sphingosine-kinase-1; siRNA, small interfering RNA; TCR, T-cell receptor; TGFβ1, transforming growth factor β1; Treg, T regulatory; TSDR, Treg-specific demethylation region; WT, wild type.**

2352-345X
http://dx.doi.org/10.1016/j.jcmgh.2014.12.007

susceptibility to colitis. The block in Treg differentiation was found to be Polycomb-mediated epigenetic silencing of the FOXP3 core promoter.[1] Extending our investigations into the entire FOXP3 regulatory region, we now report a key role for KLF14 in the maintenance of FOXP3 expression, Treg cell function, and colitis susceptibility.

KLF14, the most recent member of the KLF family to be identified, is a rapidly evolving imprinted gene with a clear function in metabolism. Indeed, recently KLF14 has been found to play a key role in lipogenesis.[3] This role in fatty acid metabolism has a profound impact in immune function, as the metabolic pathways driving T-cell differentiation fate are a novel, active area of research.[4–8] To begin to address this intersection between metabolism and immune cell fate, we have for the first time ascribed a role for KLF14 in immune function. Specifically, combined cellular, biochemical, molecular analyses, and studies in genetically engineered mice revealed a novel KLF14-mediated function in Treg cell differentiation.

At the molecular level, KLF14 mediated this phenomenon, at least in part, by transcriptionally regulating FOXP3 via a mechanism that involves methylation and chromatin remodeling of the TSDR (Treg-specific demethylation region) within the promoter of this gene. At the cellular level, KLF14 inactivation rendered Treg cells in an abnormal state of differentiation marked by their hypersuppressive phenotype in vitro and in vivo. Congruently, KLF14 knockout (KO) mice were resistant to experimentally induced colitis.

These results assign for the first time a role for KLF14 in immune cell differentiation and chronic intestinal inflammation. These data also extend our understanding of molecular mechanisms that regulate Treg cell function, a population that is altered in many disease states.

Materials and Methods

Transfection Assays

For small interfering RNA (siRNA) experiments, 300 nM siRNA was used (ONTARGET plus siRNA; Dharmacon/Thermo Scientific, Lafayette, CO). The cell-stimulation conditions included plate-bound CD3 (2 μg/mL), soluble anti-CD28 (2 μg/mL; BD Biosciences, San Jose, CA), and human interleukin-2 (100 μ/mL) and human transforming growth factor β1 (TGFβ1, 5 ng/mL) in complete RPMI media (both cytokines: PeproTech, Rocky Hill, NJ).

Isolation of Primary T Cells

Male mice were used for all experiments. Murine naïve $CD4^+$ splenocytes were isolated using a combination of magnetic separation kits (Miltenyi Biotec, Bergisch Gladbach, Germany). Sequential use of the $CD4^+CD25^+$ regulatory T cell isolation kit and the $CD4^+CD62L^+$ T cell isolation kit resulted in naïve FOXP3-negative T cells used for in vitro induction of FOXP3.

Cell Stimulation

In vitro activation of the isolated T cells followed similar conditions among the different cell types. Anti-CD3, 145-2C11 (BD Biosciences) for the mouse T cells was plate-bound at 2 μg/mL. Soluble anti-CD28 (BD Biosciences) at 2 μg/mL plus 100 units/mL interleukin-2 was added to the cultures throughout the incubation period. Human TGFβ1 recombinant (PeproTech) at a concentration of 5 ng/mL was used to generate adaptive Treg cells. The media were replaced every 3 days with cells plated into new wells coated with anti-CD3 as described previously.

Suppression Assays

For the suppression assays, $CD4^+CD25^{++}$ cells were sorted from splenocytes, using anti-CD4/anti-CD25 conjugated beads (Miltenyi Biotec), as previously described elsewhere.[9] Mixed leukocyte reactions were performed using 1×10^4 $CD4^+CD25^-$ T responder cells and 1×10^4 irradiated (3300 rads) T-cell-depleted antigen-presenting cells isolated from the same animals. Treg cells were added to the cell culture at titrations of 1:12 to 1:1. The culture medium was complete RPMI supplemented with 10% fetal bovine serum and 2.5 μg/mL anti-CD3 (UCHT1) and anti-CD28 (BD Biosciences) at 2 μg/mL. Proliferation was read at 4d upon addition of 1 μCi tritiated thymidine for the last 18 hours of culture.

RNA Isolation, cDNA Synthesis, and Quantitative Real-Time Polymerase Chain Reaction

Total RNA was isolated using the manufacturer protocol in the RNeasy Mini Kit (Qiagen, Valencia, CA). The cDNA was synthesized from 0.5–1 μg of total RNA with random primers using the SuperScript kit III First-Strand (Invitrogen/Life Technologies, Carlsbad, CA). We used 2 μL of reverse-transcription products for each real-time polymerase chain reaction (PCR). The PCRs were in 20 μL of total volume that contained primers and 10 μL of Express SYBR green ER quantitative PCR Supermaster mixes (Invitrogen). Of note, KLF14 is an intron-less GC rich gene not optimal for real-time PCR. Thus, for semiquantitative real-time PCR, genes of interest were amplified under the following conditions: initial denaturation, 95°C for 3 minutes, followed by 34 cycles with denaturation at 95°C for 30 seconds, annealing at 55°C for 60 seconds, and extension at 72°C for 60 seconds. All the PCR products were visualized by running 1.5% agarose gels electrophoresis and ethidium bromide staining for the pictures.

The following primers were used. The Foxp3 core promoter chromatin immunoprecipitation (ChIP) primers for gels were 5′-TTCAGATGACTTGTAAAGGGCAAAG and 3′-GAGAAGAAAAACCACGGCGTGGGAG. The Foxp3 TSDR ChIP primers for gels were 5′-AACCTTGGGCCCCTCTGGCA and 3′-GGCCGGATGCATTGGGCTTCA. The KLF14 primers were 5′-TCAACTAGCTGCTTCGAGCC and 3′-ACGACCTCGGTACTC GATCA. The Foxp3 primers were 5′-TTCAGATGACTTGTA AAGGGCAAAG and 3′-GAGAAGAAAAACCACGGCGTGGGAG.

Western Blot Analysis

Protein was extracted from whole-cell lysates derived from freshly isolated Treg cells and non-Treg cells. The cells were lysed Laemmli sample buffer. Protein (20 μg) was run

on 10% gel over 1 hour at 100 Amps. Upon transfer to nitrocellulose, the membrane was incubated with anti-Foxp3 (Abcam, Cambridge, MA) in 5% milk for 1 hour. Foxp3 protein was detected with 1/1000 dilution of anti-rabbit-horseradish peroxidase conjugate and an electrochemiluminescence detection kit (SuperSignal West Femto Chemiluminescent Kit; Pierce Biotechnology, Rockford, IL). The exposed films were scanned, and the digitized images were analyzed using the software VisionWorks (UVP, Upland, CA). The protein signals were indexed by measuring their relative mean grey value per area.

Chromatin Immunoprecipitation Assays

The ChIP assays were performed using a ChIP isolation kit (Millipore, Billerica, MA). We treated 1×10^5 to 5×10^5 murine naïve T cells with 1% formaldehyde to cross-link histones to DNA. The fixed cells were sonicated to yield chromatin fragments of 200–500 base pairs (bp). The antibodies used in the ChIP assays included: H3Ac (Millipore), H4Ac (Upstate Biotechnology, Lake Placid, NY), H3K9Ac (Active Motif, Carlsbad, CA), H3K4Me3 (Millipore), H3K4Me2 (Abcam), H3K4Me (Millipore), H3K9Me2 (Millipore), H3K9Me3 (Abcam) H3K27me2 (Abcam) H3K27me3 (Millipore), p300 (Abcam), PCAF (Abcam), SUV39H1 (Millipore), CBP (Abcam), ESET/SetDB1(Millipore), Ezh2 (Cell Signaling Technology, Beverly, MA), G9a/EHMT2 (C6H3) (Abcam), HP1α (Millipore), HP1β (Active Motif), and HP1γ (Millipore). DNA was recovered by a Chelex 10% slurry and sample boiling method,[10] or using the IP-STAR (Diagenode, Denville, NJ) direct chip protocol followed by the IPPURE DNA purification. 1% Pre-enriched chromatin (input) served as the percentage input for sample quantification, confirmed by fold over IgG changes. The UV-exposed 4% agarose gels were imaged, and the digitized images were analyzed using the software VisionWorks (UVP). Protein signals were indexed by measuring their relative mean grey value per area.

Adenoviral Transduction

Naïve T cells isolated from the Coxsackie adenovirus receptor (CAR) transgenic Balb/cJ[Tg],CARdelta1-[Tg] DO11.10 mice were activated for 48 hours with either empty vector (EV) or KLF14 at a multiplicity of infection of 250. The cells were activated under the typical stimulation conditions for 2 days and processed through mRNA expression.

Mouse Strains

C57BL/6J mice and C57BL/6J RAG-1 mice (recombinase activating gene-1-deficient) were initially purchased from the Jackson Laboratory (Bar Harbor, ME) and bred in conventional housing in the Mayo Clinic animal facility (Rochester, MN). The CAR transgenic mouse was obtained through the National Institute of Allergy and Infectious Diseases Exchange Program of the National Institutes of Health: Balb/cJ[Tg]CARdelta1-[Tg]DO11.10 mouse line 4285.[11] The CAR mouse expresses the Coxsackie adenovirus receptor transgene and is optimal for adenoviral transduction studies in resting lymphocytes. The KLF14$^{-/-}$ mice were kindly provided by Dr. Raul Urrutia (Mayo Clinic, Rochester, MN).[12] All the mice used in experiments were males of 4–20 weeks in age. The mice were age-matched in experiments comparing wild type (WT) with KLF14$^{-/-}$. All animal work was done in accordance with the Mayo Clinic Institutional Animal Care and Use Committee.

Dextran Sodium Sulfate Colitis

The mice were given water supplemented with 3% dextran sulfate sodium salt for 5 days. The water was then replaced with normal drinking water for 3 more days before the mice were sacrificed for tissue removal for histologic analysis. Flow cytometry was used to look at levels of FOXP3 expression within the CD4$^+$ population. Intracellular staining procedures for FOXP3 were followed using the application notes from Alexa Fluor 488 anti-mouse/rat/human FOXP3 (BioLegend, San Diego, CA).

The mice were weighed every other day, and their colon lengths were determined during autopsy. The degree of colitis was quantified using three outcome variables: weight loss, colon histology, and a disease activity index. The disease activity index is an established clinical index of colitis severity encompassing clinical signs of colitis (wasting and hunching of the recipient mouse and the physical characteristics of stool) and an ordinal scale of colonic involvement (thickness and erythema).[13] We adapted an existing histology damage score for the dextran sodium sulfate (DSS) colitis model.[14] This score assesses eight parameters, including the extent of crypt loss, depth of erosions/ulcers, and semiquantitative assessment of inflammatory cells. We added one additional parameter: extent of re-epithelialization when erosions/ulcers were present/expressed as ratio of re-epithelialized ulcer to nonepithelialized ulcer.

T-Cell Transfer Model of Chronic Colitis

Chronic colitis was induced via adoptive transfer of naïve CD4$^+$CD45RB^{high} T cells derived from WT donors using our previously published method.[15] Briefly, spleens were removed from donor WT C57BL/6J mice and macerated between the frosted ends of two microscopy glass slides to produce single-cell suspensions in phosphate-buffered saline (PBS) supplemented with 0.1% fetal bovine serum. The CD4$^+$ T cells were enriched by negative selection using magnetic beads (Miltenyi Biotec). The enriched T cells were labeled with anti-CD45RB and anti-CD25 (BioLegend) and sorted for CD45RB^{high} CD25^{low} with a FACS Aria (fluorescence-activated cell sorting; BD Biosciences). We injected 3×10^5 cells suspended in 100 μL of PBS intraperitoneally into C57BL6J RAG-1 KO animals. After 14 days, the CD25^{++} cells were isolated using CD4$^+$CD25$^+$ regulatory T cell isolation kit (Miltenyi Biotec) as described by the manufacturer's suggested protocol from the spleens of either WT C57BL/6J or KLF14 KO mice. These cells were subjected to a second magnetic column and washing step at the CD25$^+$ step to further purify the regulatory T-cell population (greater than 95% FOXP3$^+$ in

WT or KLF14 KO mice, data not shown). We suspended 7.5×10^4 cells in 100 μL of PBS, which was injected intraperitoneally into animals that had undergone adoptive transfer of $CD4^+CD45RB^{high}$ WT T cells 2 weeks earlier. The animals were switched to nonirradiated chow, and their weight was recorded every other day. The Mayo Clinic Animal Facility, unless specifically directed, only uses autoclaved and irradiated chow, but nonirradiated chow frequently is required to induce robust colitis in this model.[16] The histologic disease activity was assessed by our participating gastrointestinal pathologist who was blinded to the study grouping. We adapted an existing histology damage score for the T-cell transfer colitis model.[15] This score assesses eight parameters, including extent of crypt loss, depth of erosions/ulcers, and semiquantitative assessment of inflammatory cells.

RNAseq of Human Samples

The isolation of lamina propria $CD4^+$ lymphocytes has previously been described elsewhere.[9] Briefly, resection specimens or mucosal biopsy samples of the terminal ileum were obtained from six patients with Crohn's disease or age/sex-matched healthy controls. The tissue initially underwent mechanical disruption in the presence of 1 mM EDTA in a 37°C CO_2 incubator for 30 minutes followed by a collagenase (1 mg/mL), DNase (1 mg/mL), and trypsin inhibitor (1 mg/mL) overnight at 4°C in complete RPMI supplemented with 10% human serum. After passage through a 70-μm cell strainer, the buffy coat was isolated using Ficoll gradient centrifugation. The $CD4^+$ lamina propria cells were isolated using magnetic bead sorting ($CD4^+$ T Cell Isolation kit, 130–091–155; Miltenyi Biotec) and two passes through the LS column on the MACS magnetic separator. Purification was confirmed by flow cytometry.

Sequencing data was analyzed using the processed paired-end mRNA sequencing analysis using the MAP-RSeq v1.2.1.3 workflow (Mayo Clinic, Rochester, MN). This analysis provided gene and exon level expression. We performed differential expression analysis using edgeR (Bioconductor, Bioconductor.org) for the following disease versus control.

Statistical Methodology

Statistical analyses were performed using JMP version 9.0 (SAS Institute, Cary, NC). Nonparametric unpaired *t* test was performed using the Mann-Whitney *t* test, and $P < .05$ was considered statistically significant. For multiple comparisons, statistical significance was determined using the Holm-Sidak method, with alpha = 5.000% ($P < .05$). Each variable was analyzed

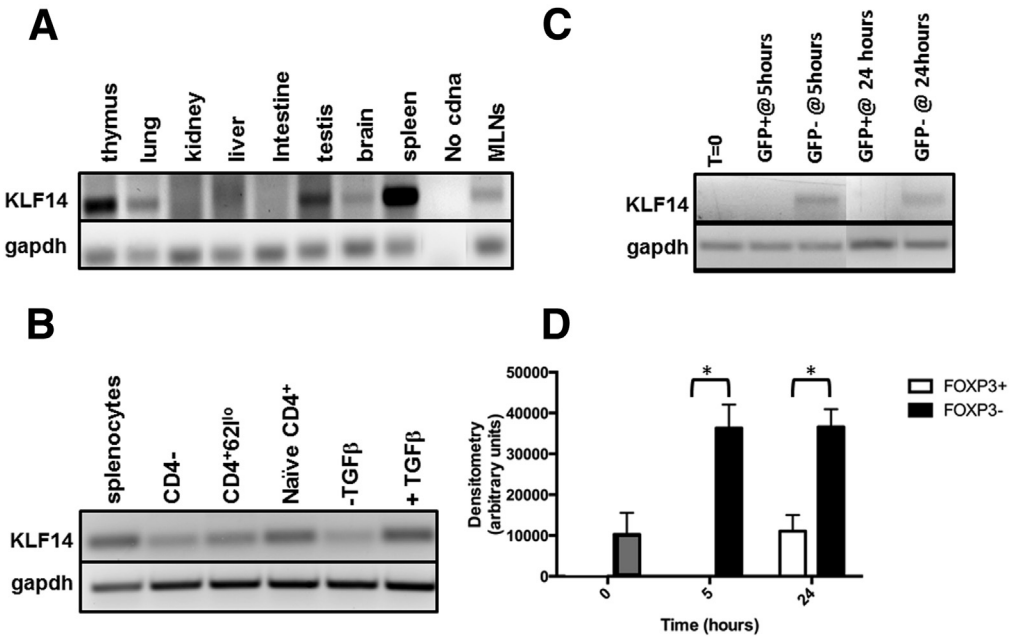

Figure 1. KLF14 is present in the immune compartment and induced by transforming growth factor β1 (TGFβ) in vitro in FOXP3-negative lymphocytes. (*A*) DNA gel for polymerase chain reaction (PCR) analysis of the expression of KLF14 in mouse tissues. The data are a representative figure of three independent experiments. (*B*) DNA gel for PCR analysis of the expression of KLF14 in splenocyte subsets. Note the enhanced expression of KLF14 in $CD4^+$ lymphocytes (*right four panels*) and $CD4^+$ lymphocytes stimulated with TGFβ (*far right column*). The housekeeping gene *gapdh* is provided as loading control (*lower row*). The data are representative of three independent experiments. (*C, D*) DNA gel for PCR analysis of the expression of KLF14 in $CD4^+$ cells activated to induce FOXP3. Note that KLF14 expression segregates to GFP (surrogate for FOXP3) negative cells at all time points. (*D*) Histogram representing the optical density of gel bands. Note that time 0 (*grey bar*) represents unstimulated cells. The data are representative of three independent experiments. Statistical significance was determined using the Holm-Sidak method of multiple comparisons, with alpha = 5.000% ($P < .05$). Each time point was analyzed individually, without assuming a consistent standard deviation.

individually, without assuming a consistent standard deviation (SD).

Results

KLF14, Present in Immune Cells, Is Inversely Associated With FOXP3

The expression pattern of KLF14 in immune tissue is currently unknown, precluding us from inferring any potential function of this protein in the immune system. Consequently, we performed an expression analysis from various murine tissue extracts to gain insight into the spatial distribution of this transcription factor. KLF14 mRNA was ubiquitous in murine tissues, with particularly strong expression in primary and secondary lymphatic organs (Figure 1*A*).

Within the spleen, KLF14 expression segregated to $CD4^+$ lymphocytes, a finding that suggested a putative role for KLF14 in the differentiation of $CD4^+$ T helper phenotypes (Figure 1*B*). We stimulated naïve $CD4^+$ lymphocytes into adaptive Treg cells (see *Materials and Methods*) and measured KLF14 expression (Figure 1*B*). After 72 hours of activation, KLF14 was induced by TGFβ1 and up-regulated within the entire population of $CD4^+$ cells (right column, Figure 1*B*). Upon separation of $CD4^+$ cell subsets based upon FOXP3 expression, we demonstrated an inverse relationship between FOXP3 and KLF14 (Figure 1*C* and *D*). Together, these studies demonstrate that KLF14, enriched in immune organs and cells is induced during the initial differentiation of naive lymphocytes to adaptive Treg cells; however, KLF14

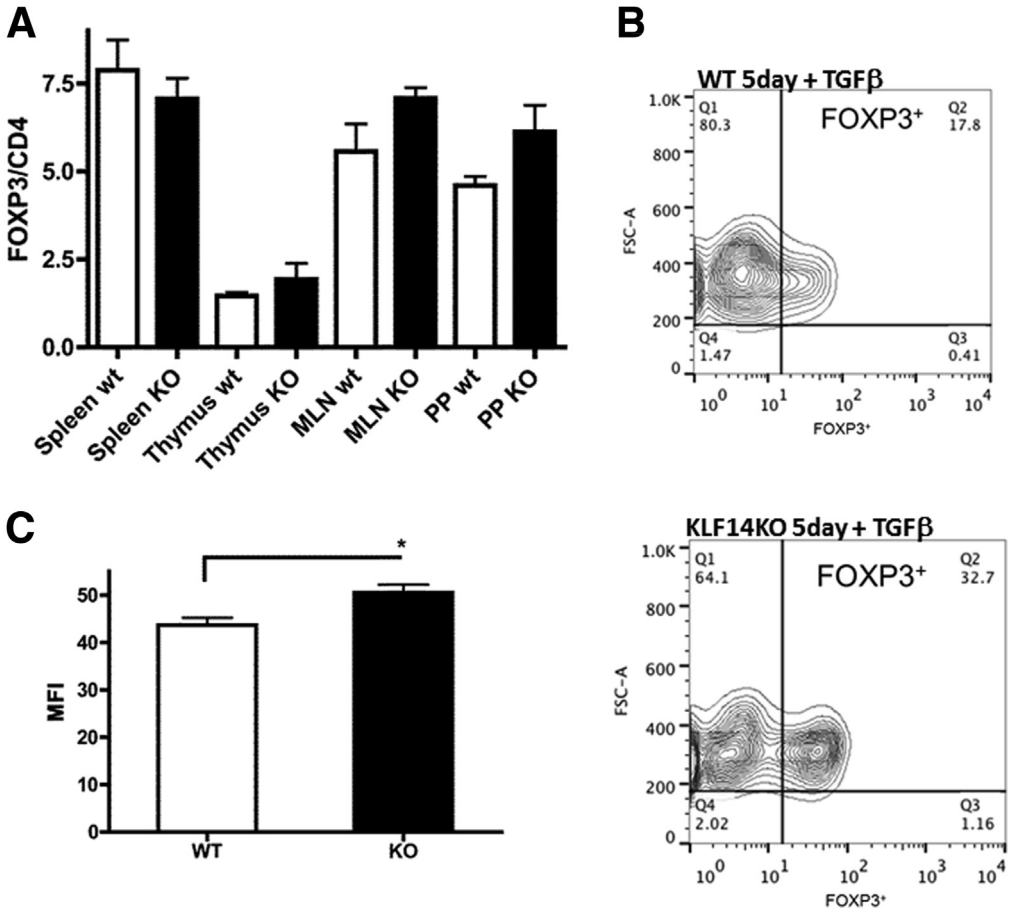

Figure 2. KLF14 deficiency in $CD4^+$ lymphocytes results in up-regulation of FOXP3. (*A*) Flow cytometry for FOXP3, expressed as a percentage of $CD4^+$ cells in central and peripheral lymphatic organs. Note the numerical difference in $FOXP3^+$ cells within gut-associated lymphoid organs (mesenteric lymph nodes [MLN] WT vs KLF14 KO, 5.6% $\pm$ 0.8% vs 7.1% $\pm$ 0.3%; Peyer's patches [PP] WT vs KLF14 KO, 4.6% $\pm$ 0.3% vs 6.1% $\pm$ 0.7%). The data represent the mean/standard error of the mean of five WT and 5 KLF14 KO mice. A nonparametric, unpaired *t* test of significance between lymphoid organs (Mann-Whitney) demonstrated no statistically significant difference. (*B*) Flow cytometry for FOXP3 in $CD4^+$ lymphocytes stimulated for 5 days with T-cell receptor (TCR) and transforming growth factor β1 (TGFβ). Note the enhanced expression of FOXP3 (32.7% vs 17.8%, KLF14 KO vs WT) in KLF14-deficient T cells. The data are representative of three independent experiments. (*C*) Mean fluorescent intensity for FOXP3 (FL-1 channel) in induced T regulatory (Treg) cells. Note the significantly higher mean fluorescent intensity in KLF14 KO in the in vitro differentiated Treg cells (50.5 $\pm$ 1.7 vs 43.7 $\pm$ 1.5, KLF14 KO vs WT, $P = .04$). The results represent the mean/standard error of the mean fluorescent intensity of three independent experiments. A nonparametric, unpaired *t* test of significance between WT and KLF14 KO (Mann-Whitney) demonstrated statistical significance ($P < .05$).

segregates to the FOXP3 population in vitro. These results led us subsequently to investigate the impact of KLF14 gene deletion on the biological responses of differentiated Treg cells.

Expression of KLF14 Is Inversely Correlated With FOXP3 Expression and Function In Vivo

A survey of the principal immune components of the KLF14 KO mouse demonstrates a normal CD4:CD8 ratio and normal populations of $CD19^+$ and $CD11b^+$ cells (B cell and myeloid lineage, respectively) within the spleen when compared with age- and sex-matched control mice (Supplementary Figure 1). We did observe numerically higher but not statistically significantly different percentages of $FOXP3^+$ cells (expressed as a percentage of $CD4^+$ lymphocytes) in mucosal-associated lymphoid tissue (mesenteric lymphatic nodes [MLN] and Peyer's patches [PP], Figure 2*A*).

Upon stimulation of naïve $CD4^+$ splenocytes to differentiate into adaptive Treg cells (see *Materials and Methods*), we observed a higher frequency of $FOXP3^+$ cells in vitro in the absence of KLF14 (Figure 2*B*). Furthermore, intracellular expression of FOXP3 is enhanced as assessed by mean fluorescent intensity in KLF14 KO Treg cells (Figure 2*C*). Enhanced differentiation into $FOXP3^+$ T cells in the absence of KLF14 was not due to altered kinetics of cellular proliferation, as naïve lymphocytes from WT or KLF14 KO mice proliferated equally as assessed by fluorescence-activated cell sorting and intracellular dye dilution (Supplementary Figure 2). Similar proliferation between WT and KLF14 KO cells was seen in both $FOXP3^+$ and FOXP3- cell populations (Supplementary Figure 3).

To study the functional relevance of this in vitro finding, we evaluated mucosal immune response to DSS. Although not specific for adaptive immune cell function, the DSS-induced colitis model is a well-established tool to study mucosal inflammation in genetically engineered mice, including those deficient in KLF proteins.[1] Thus, we assessed the development and severity of colitis by DSS in KLF14 KO mice by measuring weight loss, colon length, disease activity index, and histopathology. Interestingly, we found that upon DSS treatment, KLF14 KO mice displayed statistically significantly less weight loss (28.0 ± 1.1 g vs 23.5 ± 0.99 g, $P = .001$), reduced colonic shortening (6.8 ± 0.6 cm vs 4.9 ± 0.5 cm, $P = .0007$), and lower clinical disease activity scores as compared with the WT control animals (0.69 ± 0.73 vs 2.13 ± 0.86, $P = .02$) (Figure 3*A*–*C*).

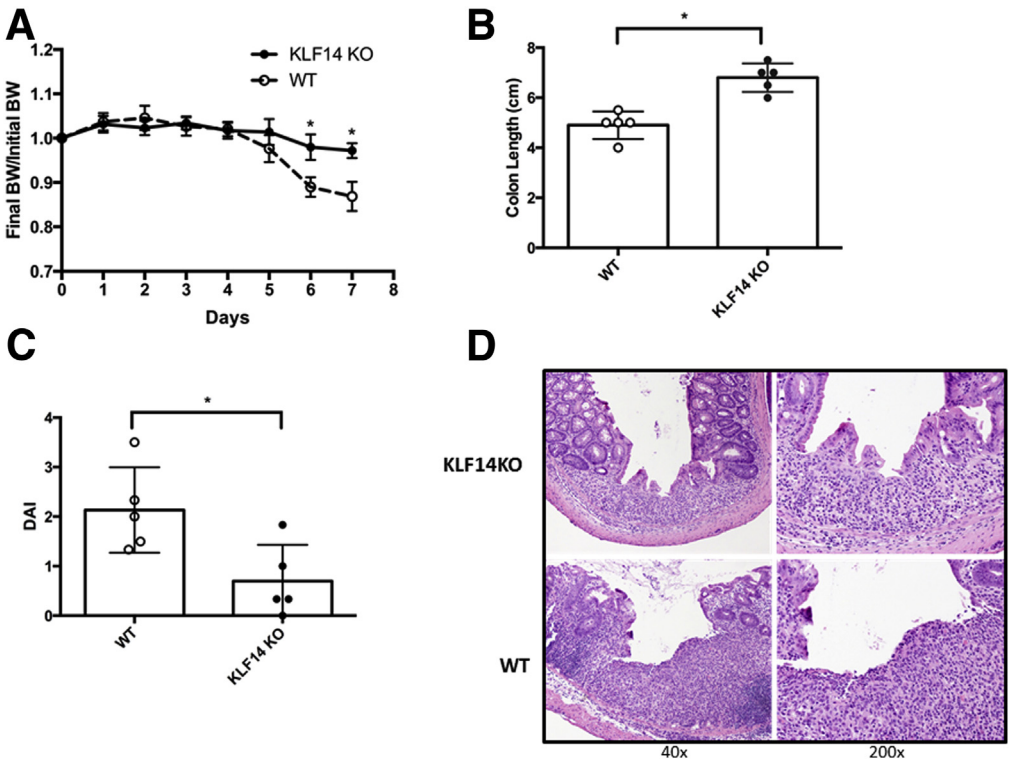

Figure 3. KLF14 KO animals are resistant to dextran sodium sulfate (DSS) colitis. Tabulation of (*A*) weight change, (*B*) colon length, (*C*) clinical disease activity scores, and (*D*) histologic disease in DSS-exposed mice demonstrates significantly less severe colitis in KLF14-deficient (*closed circles*) versus wild type (WT) (*open circles*) animals. (*D*) Representative histologic section from the colon of a KLF14-deficient mouse compared with the significant inflammation and ulceration demonstrated in the colon of a WT mouse (*D*). Statistical significance for weight change was determined using the Holm-Sidak method, with alpha = 5.000% ($P < .05$). Each time point was analyzed individually, without assuming a consistent standard deviation. For colon length and disease activity index, significance was determined using a nonparametric, unpaired *t* test of statistical significance (Mann-Whitney), $P < .05$. The data are representative of three experiments, n = 5 mice per group.

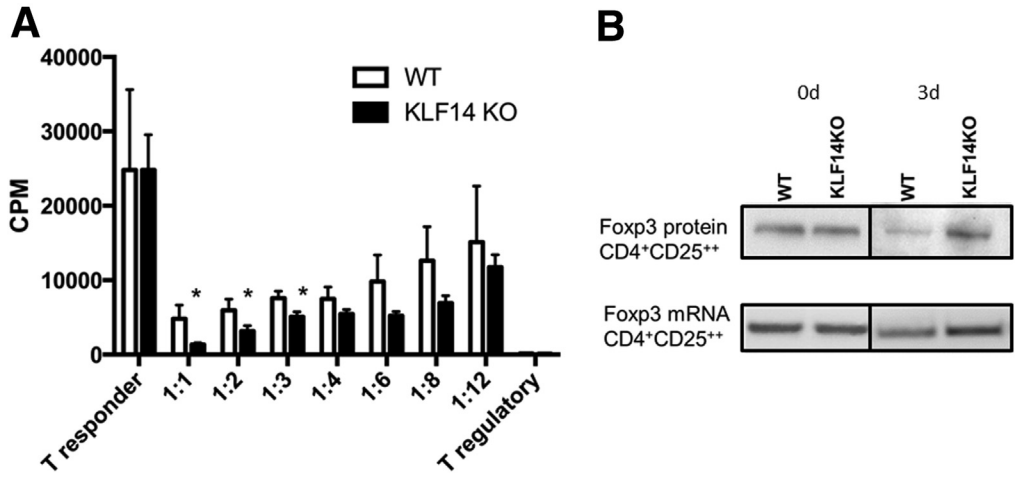

Figure 4. KLF14-deficient T regulatory (Treg) cells demonstrate enhanced suppression in vitro. (*A*) Histogram representing thymidine incorporation of T-responder cells in coculture with T-regulatory cells isolated from wild-type (WT) (*white columns*) or KLF14 knockout (KO) mice (*black columns*). Note the enhanced suppression of proliferation across all titrations, significantly so upon higher titration ratios (WT vs KLF14 KO: 7595 ± 906 vs 5099 ± 647, 1:3; 5948 ± 1488 vs 3158 ± 716, 1:2; 4804 ± 1833 vs 1349 ± 223, 1:1, $P < .05$). Presented are the mean and standard deviation (SD) of thymidine counts conducted in triplicate. Data are representative of three independent experiments. Statistical significance was determined using the Holm-Sidak method, with alpha = 5.000% ($P < .05$). Each titration was analyzed individually, without assuming a consistent SD. (*B*) Enhanced in vitro suppression of KLF14-deficient Treg cells associated with greater expression of FOXP3. Demonstrated is the immunoblot analysis (*upper row*) and DNA gel (*lower row*) for FOXP3 protein (*upper*) and mRNA (*lower*) in Treg cells after 3 days of suppression assay culture. Note the heightened expression of FOXP3 in KLF14 KO cells compared with WT. Data are representative of three independent experiments.

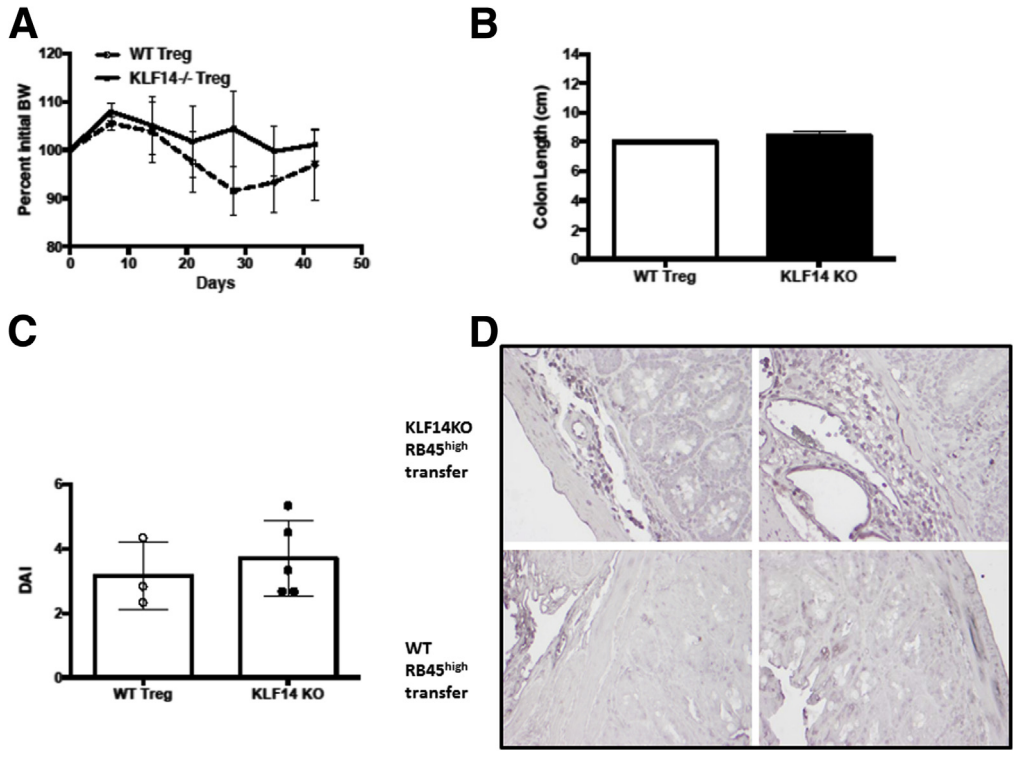

Figure 5. KLF14 knockout (KO) T-effector cells induce colitis. Tabulation of (*A*) weight change, (*B*) colon length, and (*C*) clinical disease activity scores in CD45Rb^{high} transferred RAG recipients. Results demonstrate equivalently severe colitis in RAG recipients of KLF14 KO (*closed circles* or *histogram*) and wild-type (WT) (*open circles* or *histogram*) CD45Rb^{high} T cells. (*D*) Representative histologic sections from the colon of a recipient of KLF14 KO T cells (*top panel*) compared with the colon of a recipient of WT T cells (*lower panel*). Immunohistochemical analysis for FOXP3 demonstrates the presence of FOXP3^{+} lymphocytes in recipients of KLF14 KO T cells. Data from n = 10 mice, 5 per treatment group (mean and standard deviation). A nonparametric, unpaired *t* test of significance between genotypes (Mann-Whitney) demonstrated no statistically significant difference.

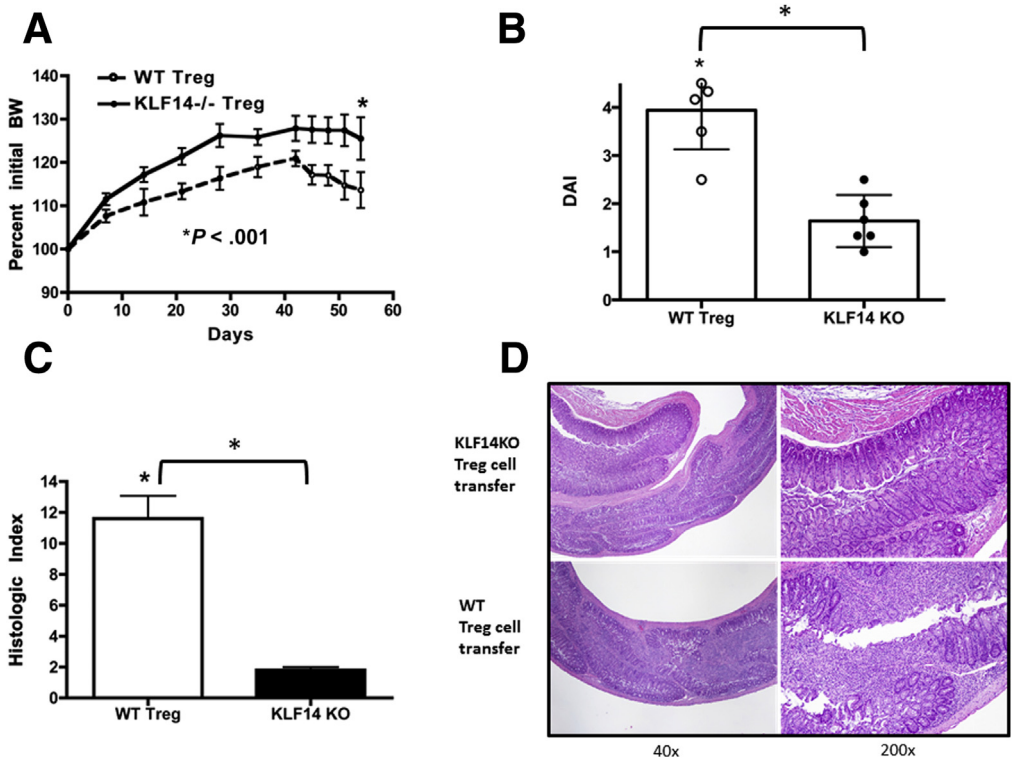

Figure 6. KLF14-deficient T regulatory (Treg) cells demonstrate enhanced suppression in vivo. Tabulation of (*A*) weight change, (*B*) clinical disease activity scores, and (*C*) histologic disease activity index in CD45Rb^{high} transferred RAG recipients after treatment with WT or KLF14 KO Treg cells. The results demonstrate significantly less severe colitis in recipients of KLF14-deficient (*closed circles* or *histogram*) versus wild-type (WT) (*open circles* or *histogram*) Treg cells. (*D*) Representative histologic sections from the colon of a recipient of KLF14 KO Treg cells compared with the significant inflammation and ulceration demonstrated in the colon of a recipient of WT Treg cells. Statistical significance for weight change was determined using the Holm-Sidak method, with alpha = 5.000% ($P < .05$). Each time point was analyzed individually, without assuming a consistent standard deviation (SD). For the disease activity index and histologic activity index, statistical significance was determined using a nonparametric, unpaired *t* test of significance (Mann-Whitney), $P < .05$. Data from n = 10 mice, 5 per treatment group (mean and SD, *$P < .05$).

The development of colonic inflammation was confirmed by blinded histologic examination of the colons. In comparison with the WT control animals, the colon of the DSS-treated KLF14 KO mice contained fewer inflammatory cells, reduced ulceration (11.4% ± 4.17% vs 30.7% ± 8.8%, $P = .02$, for n = 7 animals), and enhanced re-epithelialization (83.3% ± 28.8% vs 36.2% ± 6.5%, $P = .02$, for n = 7 animals; Figure 3*D*). These observations demonstrate that genetic inactivation of KLF14 in the germ line confers protection from experimental colitis. We recognize the

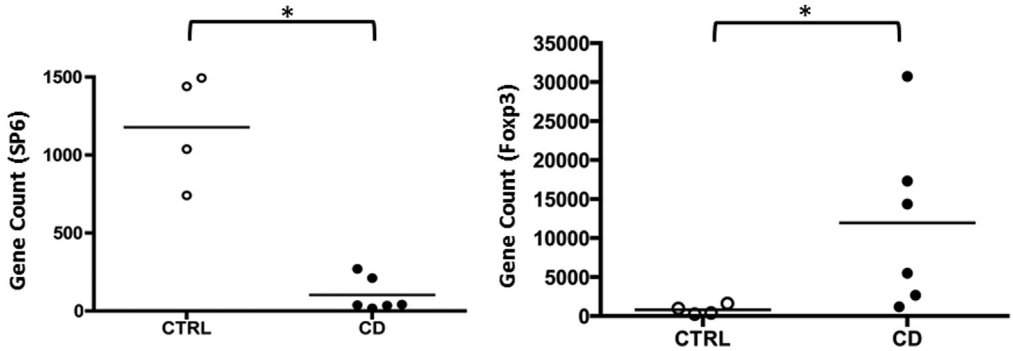

Figure 7. SP6 (KLF14) is inversely associated with Foxp3 in CD4$^+$ cells isolated from patients with Crohn's disease. We performed gene expression analysis on CD4$^+$ cells isolated from affected (CD, *closed circles*) and unaffected tissue (CTRL, *open circles*). Note the inverse relationship between FOXP3 and KLF14 (n = 10 subjects, $P < .05$). A differential expression analysis using edgeR for disease versus control at a false-discovery rate of <0.05 was used.

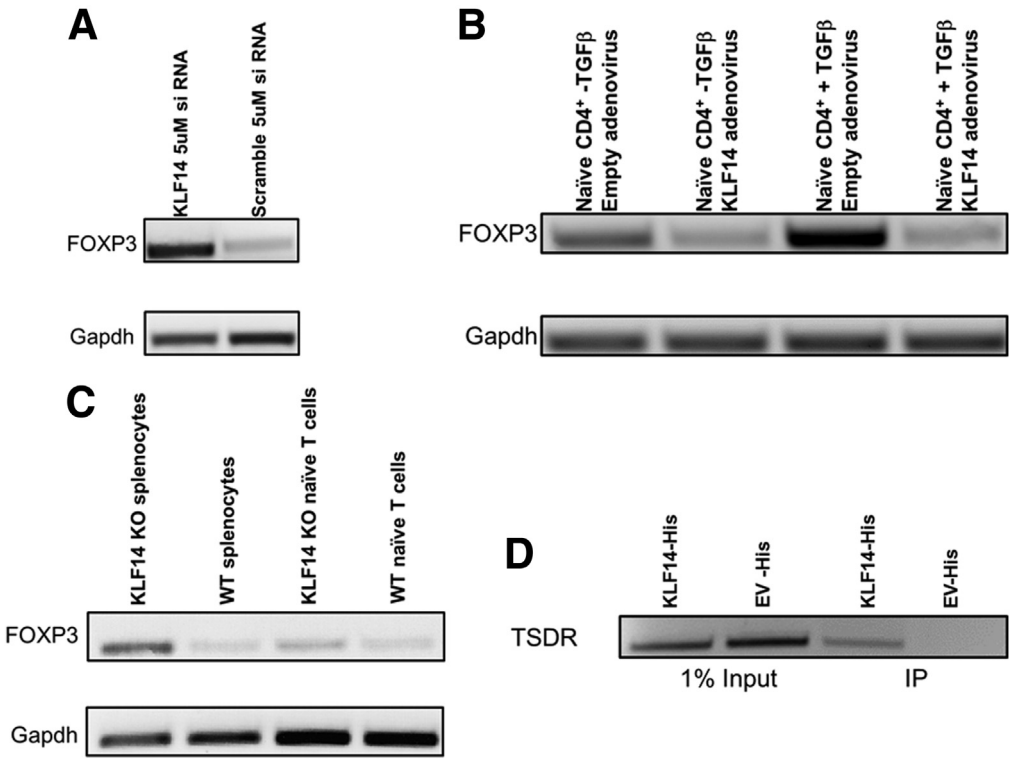

Figure 8. KLF14 binds to the TSDR (Treg-specific demethylation region) and is a transcriptional regulator of FOXP3. DNA gels for polymerase chain reaction (PCR) analyses of expression of FOXP3 in naïve $CD4^+$ lymphocytes after siRNA knockdown (KO) (*A*) or adenoviral overexpression (*B*) of KLF14. Note that knockdown of KLF14 leads to enhanced FOXP3 expression (*A*) whereas overexpression, particularly in the setting of transforming growth factor β1 (TGFβ) stimulation, leads to repression of FOXP3 (*B*). Similarly, freshly isolated splenocytes and naïve $CD4^+$ lymphocytes from the KLF14 KO animal demonstrate enhanced FOXP3 expression when compared with the wild type (WT) (*C*). Data are representative of three independent experiments. (*D*) DNA gel for PCR using primers specific for the TSDR within the FOXP3 locus in samples after precipitation for KLF14-His in murine naïve $CD4^+$ splenocytes after overexpression with either KLF14-His or empty vector (EV). Note the ready identification of KLF14 at the TSDR as compared to the empty vector control. Data are representative of three independent experiments.

shortcomings of the DSS acute colitis model, particularly in its lack of specificity for adaptive immune cells, so we focused further study of KLF14 and colitis in T-cell-dependent assays.

We next tested the in vitro suppressor function of isolated Treg cells from both WT and KLF14 KO animals against titrated T-responder cells (Figure 4*A* and Supplementary Figure 4). The results of these experiments demonstrated an enhanced KLF14 KO Treg cell suppressor function (counts per minute 1349 ± 223.2 vs 4804 ± 1833.2, $P = .03$; KL14 KO vs WT at 1:1 ratio). The suppression assay was performed using alternatively syngeneic T-responder cells (Figure 4*A*) and a common T-responder cell population (Supplementary Figure 4) with equivalent results. As the cellular abundance of FOXP3 correlates with function,[17,18] we quantified FOXP3 in WT and KLF14 KO Treg cells in cell culture conditions established for the suppression assay. Figure 4*B* shows that deletion of KLF14 increased the expression of FOXP3 at both the protein (top row, Figure 4*B*) and the mRNA level (bottom row, Figure 4*B*).

Subsequently, we tested the in vivo suppressor function of KLF14 KO Treg cells. We used the $CD4^+CD45RB^{high}$ T cell into RAG KO (Rb^{high} transfer) model of colitis.[19] To rule out an effect of KLF14 in the T-effector cells in vivo, we first performed a Rb^{high} transfer using naïve cells from WT or KLF14 KO donor mice. The transfer of naïve $CD4^+$ T cells from both WT and KLF14 KO donor mice resulted in equally severe colitis (Figure 5). In support of our previous in vitro data of enhanced conversion of naïve T cells to Treg cells in the absence of KLF14, we did detect more $FOXP3^+$ cells within the colon of recipients of KLF14 KO T cells when compared to WT by immunohistochemical analysis (Figure 5).

Next, to directly test the in vivo function of KLF14 KO Treg cells, we performed adoptive transfer of WT or KLF14 KO Treg cells into mice with established disease. Treg cells were isolated from the spleens of WT or KLF14 KO mice after CD25 magnetic bead selection (see *Materials and Methods*). Two weeks after the $CD45Rb^{high}$ transfer of WT naïve T cells, 75,000 WT or KLF14 KO Treg cells were transferred into RAG KO recipient animals to stringently test the extraordinary in vivo Treg function. We assayed colitis in the mice by measuring weight loss, colon length, disease activity index, and histopathology. Mice rescued with KLF14 KO Treg cells experienced statistically significantly more

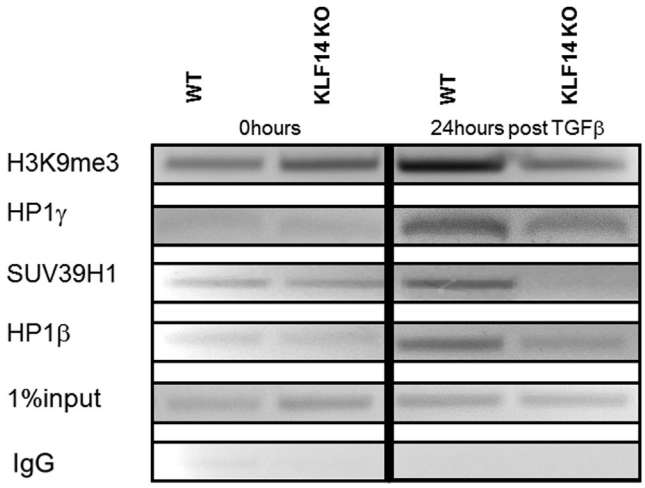

Figure 9. KLF14 associates with H3K9me3 histone marks and the corresponding histone methyltransferase complex at the TSDR. Semiquantitative polymerase chain reaction chromatin immunoprecipitation analysis of the expression of FOXP3 in cell fractions after immunoprecipitation for H3K9me3, HP1γ, SUV39H1, and HP1β in naïve T cells at $t =$ 0 hours and 24 hours after transforming growth factor β1/T regulatory (TGFβ-Treg) stimulating conditions. Note the association of H3K9me3, HP1γ, HP1β, and SUV39H1 with the wild-type (WT) but not KLF14 knockout (KO) Treg cells. The data are representative of three independent experiments.

weight gain (121.5% original weight ± 14.9% vs 103.5% original weight ± 8.1%, $P = .03$), reduced colonic shortening (8.21 ± 0.43 cm vs 7.05 ± 0.34 cm, $P = .0004$), and lower clinical disease activity scores as compared with the WT Treg-injected control animals (2.25 ± 0.80 vs 5.50 ± 1.45 $P = .0008$) (Figure 6). Furthermore, animals injected with KLF14 KO Treg cells had statistically significantly less

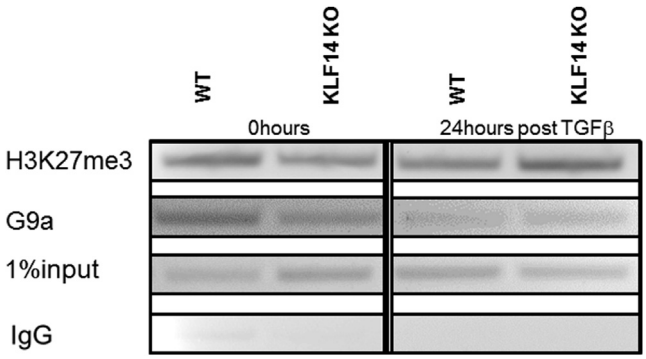

Figure 10. Lack of association with either G9a or H3K27me3 at the TSDR (Treg-specific demethylation region) in relationship to KLF14 genotype. Semiquantitative polymerase chain reaction chromatin immunoprecipitation analysis of the expression of FOXP3 in cell fractions after immunoprecipitation for H3K27me3 and G9a in naïve T cells at $t =$ 0 hours and 24 hours after transforming growth factor β1/T regulatory (TGFβ-Treg) stimulating conditions. Note there are no differences in the levels of the methlytransferase G9a or the Polycomb-associated mark H3K27me3. The data are representative of three independent experiments.

cellularity of their mesenteric lymph nodes ($4.4 \times 10^6 \pm 1.9 \times 10^6$ vs $2.2 \times 10^6 \pm 9.6 \times 10^5$, $P = .03$) than the WT Treg injected animals. The development of colonic inflammation was confirmed by blinded histologic examination of the colons. In comparison with the WT Treg-injected control animals, the colon of the KLF14 KO Treg-injected mice contained fewer inflammatory cells and reduced ulceration/erosion and crypt loss, resulting in a statistically significantly reduced histologic index of colitis (11.6 ± 3.29 vs 1.8 ± 0.45, $P = .0002$, n = 10, n = 5 animals per treatment group) (Figure 6).

Combined, our in vivo and in vitro experiments demonstrated that deletion of KLF14 results in an abnormal increase in the intracellular levels of FOXP3 and enhanced suppressive function of Treg cells in vitro and in vivo. Moreover, gene expression analysis of $CD4^+$ lymphocytes isolated from Crohn's disease intestinal lesions demonstrated KLF14 (alias SP6) to be inversely associated with FOXP3 and differentially regulated between Crohn's patients and healthy controls (Figure 7). This finding suggests a potential role for KLF14 in human inflammatory disease as well. As stable FOXP3 expression is necessary to maintain the fully differentiated state of Treg cells,[20] and epigenetic modifications of the TSDR are associated with stable FOXP3 expression, we subsequently studied the epigenetic state of the TSDR.

KLF14 Is a Transcriptional Repressor of FOXP3 Acting via the Treg-Specific Demethylated Region

Our experiments in genetically engineered KLF14 KO Treg cells revealed an inverse correlation between KLF14 and maintenance of FOXP3 expression, the master regulator of Treg cell differentiation. To rule out the possibility that the up-regulation of FOXP3 is not simply a compensatory response to the deletion of KLF14 in the germ line, we performed complimentary experiments overexpressing and knocking down KLF14. We performed acute depletion of the KLF14 mRNA using siRNA-based knockdown. The results of these experiments, shown in Figure 8*A*, demonstrated that acute depletion of KLF14 by siRNA increased FOXP3 expression.

Reciprocal overexpression experiments were performed using adenoviral transduction of KLF14 into primary naïve $CD4^+$ lymphocytes. Figure 8*B* shows that overexpression of KLF14 decreased Foxp3 expression in both resting (Naïve Ts-TGFβ1) and stimulating conditions (Naïve Ts+TGFβ1). Thus, both genetic approaches—in vivo knock out (Figure 8*C*) and in vitro knock down of KLF14—link the function of this transcription factor to the regulation of FOXP3 gene expression and maintenance.

To test whether KLF14 regulated FOXP3 directly, we performed ChIP assays in primary naive T cells. Upon adenoviral transduction of KLF14-His into primary naïve $CD4^+$ lymphocytes, we demonstrated that KLF14 bound to the FOXP3 promoter locus, and specifically within the TSDR (Figure 8*D*). Together these experiments demonstrated that KLF14 is normally bound to the TSDR during cell

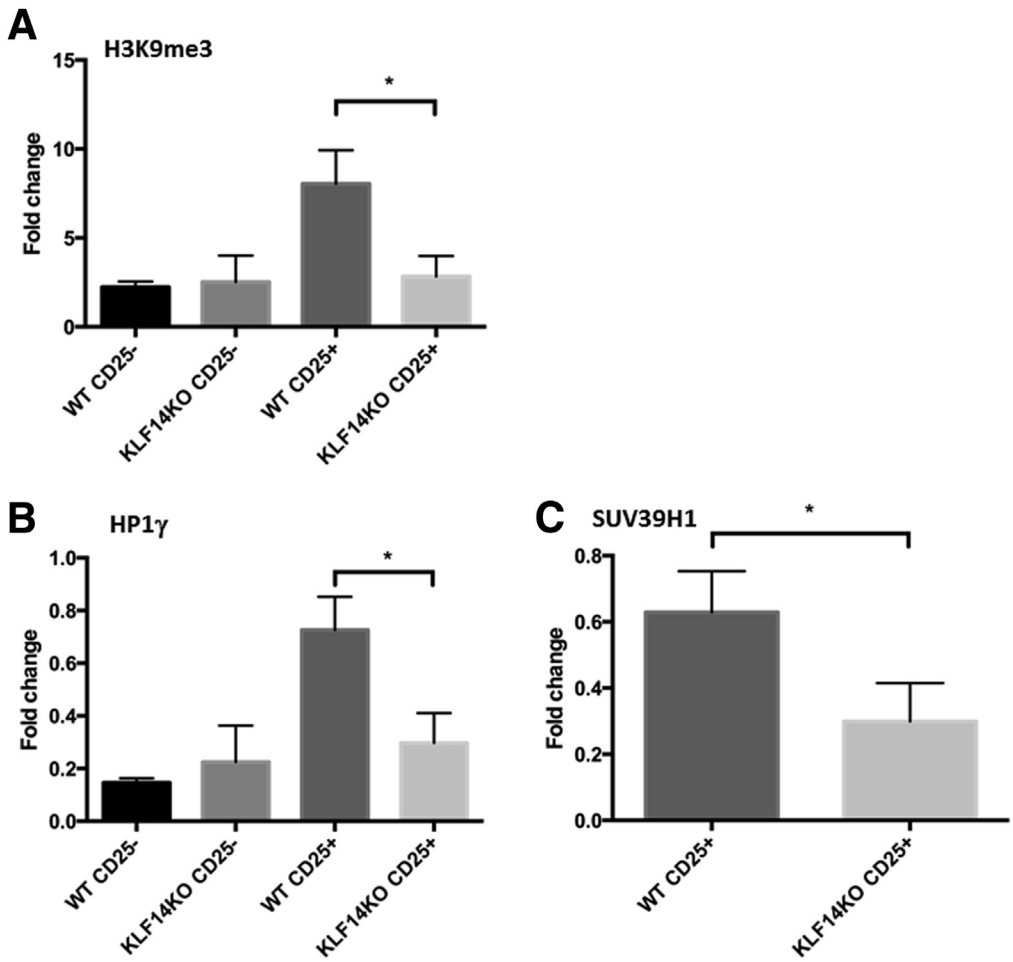

Figure 11. KLF14 associates with H3K9me3 histone marks and the corresponding histone methyltransferase complex at the TSDR in freshly isolated CD25$^+$ T regulatory (Treg) cells. Quantitative real-time polymerase chain reaction analysis of the expression of FOXP3 in cell fractions after immunoprecipitation for (*A*) H3K9me3, (*B*) HP1γ, or (*C*) SUV39H1 in primary CD4$^+$ T-cell subsets. Note the significant association of H3K9me3 (8.04 $\pm$ 1.09 vs 2.84 $\pm$ 0.65 fold change, $P < .05$), HP1γ (0.73 $\pm$ 0.07 vs 0.30 $\pm$ 0.07 fold change, $P < .05$), and SUV39H1 (0.63 $\pm$ 0.07 vs 0.30 $\pm$ 0.06 fold change, $P < .05$) with the wild-type (WT CD25$^+$) but not KLF14 knockout (KLF14 KO CD25$^+$) Treg cells. The data represent the mean/standard error of the mean of three independent experiments. Statistical significance was determined using a nonparametric, unpaired *t* test of significance (Mann-Whitney), $P < .05$.

differentiation from the naïve state to adaptive Treg cells. In the absence of KLF14, FOXP3 expression and Treg suppressor capacity were enhanced; thus, we subsequently evaluated the potential for KLF14 to regulate chromatin modification of the TSDR.

Regulation of the FOXP3 Locus by KLF14 Involves Chromatin Remodeling of the Treg-Specific Demethylated Region

It has recently been demonstrated that stable *Foxp3* expression, like the one that is observed in thymus-derived, terminally differentiated Treg cells, is marked by epigenetic modifications of the Treg-specific demethylated region (TSDR), a CpG-rich, noncoding sequence within the first intron of the *Foxp3* gene locus.[21] Based on this knowledge, we reasoned that KLF14 potentially influences FOXP3 expression by mediating changes in the levels of both histone marks and CpG island methylation within this regulatory module. Consequently, we examined whether KLF14 changes the levels of histone marks associated with nucleosomes present on the TSDR.

We performed ChIP-based analyses of this region upon differentiation of naïve CD4$^+$ lymphocytes to induce FOXP3. Of interest, stimulation over 24 hours in conditions to induce FOXP3 led to H3K9me3 marks deposited on the TSDR of WT but not KLF14 KO CD4$^+$ lymphocytes (Figure 9). Congruently, the H3K9me3 mark was associated with the responsible histone methyltransferase (SUV39H1, Figure 9) and the HP1 family of epigenetic transcriptional repressors recruited through binding to the H3K9me3 mark (HP1β, HP1γ, Figure 9).[22,23] Control experiments demonstrated that this variance in H3K9me3 levels between WT and KLF14 KO cells was accompanied by the expected inverse relationship with the preceding H3K9 dimethylation mark (Supplementary Figure 5).

Subsequent experiments evaluating additional chromatin repressor complexes demonstrated no specific

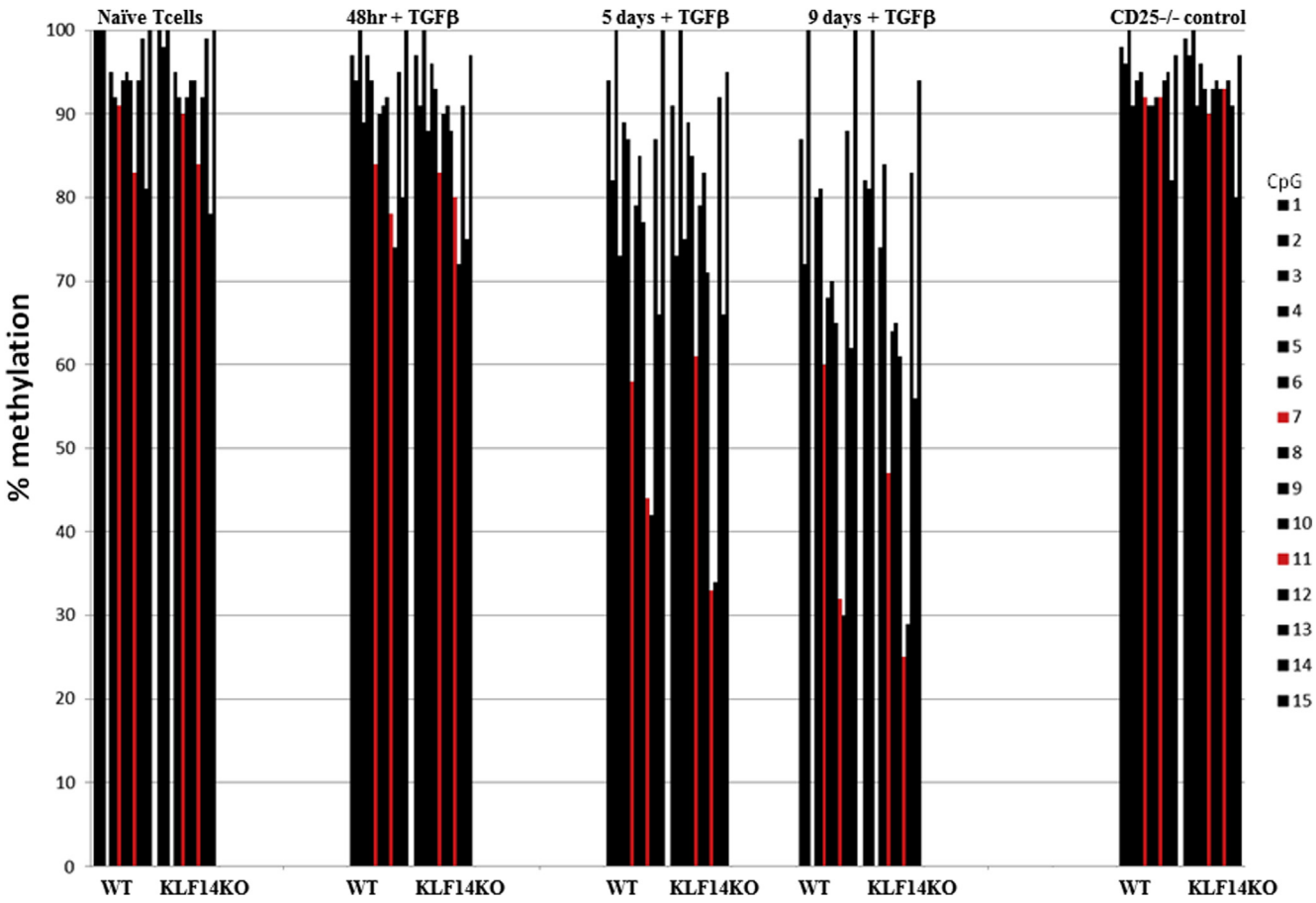

Figure 12. Pyrosequencing of the TSDR (Treg-specific demethylation region) in T-regulatory (Treg) cells from wild-type (WT) and KLF14 knockout (KO) mice during Treg differentiation. We directly measured the levels of methylation at the TSDR by pyrosequencing using genomic DNA of naïve T cells isolated from KLF14 KO and WT animals at T = 0 (naïve T cells) and after 48 hours, 5 days, and 9 days of Treg-stimulating conditions (CD25 cells used as controls). We confirmed decreasing methylation of CpG sites (labeled 1–15) within the FOXP3 TSDR over time in both WT and KLF14 KO cells. Residues 7 and 11 are demonstrated in red. Data are representative of three independent experiments.

association with the H3K9 methyltransferase G9a or additional repressor marks (H3K27me3, Figure 10). We performed confirmatory analyses of freshly isolated Treg cells from WT and KLF14 KO donor mice. Using ChIP assay and quantitative real-time PCR, we confirmed the association of the H3K9me3 marks, the HMT SUV39H1, and HP1γ with the TSDR of WT but not KLF14 KO freshly isolated Treg cells ($CD25^{+}$, Figure 11). It is established that H3K9me3 marks may lead to DNA methylation. We performed pyrosequencing of the TSDR in Treg cells from WT and KLF14 KO animals demonstrating variance in methylation of critical CpG residues (Figure 12). We conclude, that congruent with a role as a transcriptional repressor of FOXP3, deletion of KLF14 results in higher levels of expression for this target gene via a mechanism that involves, at least in part, chromatin remodeling at the TSDR.

Discussion

Kruppel-like transcription factors orchestrate complex physiologic and pathologic phenotypes by regulating selective gene expression networks through DNA binding and coupling to chromatin-remodeling enzymes. These biochemical properties are critically linked to the epigenetic reprogramming of gene expression that must occur during the functional capacitation of most cell types. During the generation of induced pluripotent stem cells, KLF4 best illustrates these KLF family properties. However, many members of the KLF family support cell differentiation in a large variety of tissues.

Relevant to our current study, several recent investigations have indicated an important role for KLF proteins in the functional regulation of immune cell types. Indeed, KLF2, KLF13, and KLF10 have been implicated in the development of T cells, B cells, and Treg cells, respectively.[24–35] However, the full repertoire of KLF proteins regulating immune cell differentiation and function has yet to be established. To begin filling this knowledge gap, our laboratory and others have been studying the role of KLF proteins in FOXP3-mediated differentiation of Treg cells, the proper execution of which is critical for the maintenance of immune self-tolerance. We observed that KLF14 is expressed at the time that induced Treg cells commence their

differentiation program. Of note, KLF14 has been associated with human inflammatory diseases, including type 2 diabetes and atherosclerosis,[36] but until now has not been specifically found to act in the immune compartment. We found KLF14 to be highly expressed within primary and secondary lymphatic organs, segregating within the $CD4^+$ lymphocytes, which suggests a putative role for KLF14 in T-helper phenotypes. One such phenotype, the $FOXP3^+$ Treg cell, is of great interest within the field of immune-mediated disease.

Mutations in Foxp3 result in the devastating and lethal immune dysregulation, polyendocrinopathy, enteropathy X-linked (IPEX) syndrome, which is characterized by an overwhelming systemic autoimmune reaction in the first year of life.[11,37–40] Indeed, point mutations of FOXP3 have been recently identified in cases of familial refractory IBD-like disease.[12] Therefore, understanding the epigenetic mechanisms regulating FOXP3 is of upmost importance.

We found KLF14 to be a repressor of FOXP3 through the epigenetic regulation of the TSDR region of the promoter locus. Incomplete data exist regarding the negative regulation of FOXP3. Genetic mutant mouse lines have suggested T-cell receptor (TCR)-dependent signaling pathways (tyrosine kinase Itk[41] and cytokine responsive genes [IRF-1]),[42] to repress FOXP3 gene transcription; however, little mechanistic information particularly relating to epigenetic events was reported. We examined the role for KLF14 in chromatin-dependent mechanisms leading to epigenetic regulation at this locus. KLF14 strongly bound the TSDR in ChIP assays; in its absence, Foxp3 expression was enhanced. Thus, we looked for its effect on the chromatin landscape at the TSDR.

Compelling evidence has established demethylation at the TSDR to be required for long-term maintenance of FOXP3 expression in Tregs.[20,43,44] However, the preceding signaling events, specifically the chromatin-mediated events leading to TSDR methylation, remain unknown. Loss of KLF14 results in reduced levels of H3K9me3 and hypomethylation at the TSDR. Interestingly, Polansky et al[45] reported of the 15 CpG motifs in the TSDR that only 6, 7, 11, and 13 are essential for FOXP3 transcriptional activity as determined by luciferase reporter analysis. In our pyrosequencing comparison of pooled KLF14 KO and WT naïve cells taken at time 0 and after 48 hours, 5 days, and 9 days of Treg-inducing conditions, we found numerical variance in CpG motifs 7 and 11. Further work into the kinetics of this process is warranted. Therefore, deletion of KLF14 at the promoter region results in higher levels of Foxp3 gene expression via a mechanism that involves chromatin remodeling at the TSDR.

Interestingly, H3K9 methylases have been previously described to repress FOXP3 through epigenetic modification of the core promoter region under the direction of the SUMO E3 ligase, PIAS-1.[46] This function was found to be relevant to natural Treg cells. Recently, the methyltransferase G9A was found to regulate T-cell differentiation during intestinal inflammation, causing a similar promotion in Treg differentiation program in its absence similar to what we find with KLF14 deficiency.[47] Our study is the first to define a role for H3K9 methylase complexes in TGFβ1-inducible adaptive Treg cells through epigenetic silencing at the TSDR. Thus, a common epigenetic regulatory complex may function to regulate both natural and adaptive Treg cells, and further research is warranted into the mechanisms of specificity of recruitment to precise FOXP3 promoter domains.

Sphingosine-kinase-1 (S1P1) has been shown to be activated by KLF14 in endothelial cells and to play important roles in T-cell trafficking[48] and thymus egress.[49,50] Of particular interest, Liu et al[5] found that S1P1 blocks the differentiation of Treg cells and that this difference was not due to proliferation of Treg cells, as we have demonstrated here. Although we cannot rule out synergistic effects of KLF14 acting indirectly through S1P1 in our system, we do show that KLF14 directly acts upon the Foxp3 locus through an epigenetic mechanism.

Given our interest in adaptive Treg cells and the TGFβ1-rich milieu of the intestine, we previously identified the mechanism leading to colitis susceptibility in KLF10 KO mice to result from Polycomb-mediated epigenetic silencing of FOXP3. As opposed to the block in adaptive Treg generation in the KLF10 KO mouse,[1,2] the lymphocytes from the KLF14 KO mouse readily convert to adaptive Treg cells and demonstrate enhanced suppressor function in vitro and in vivo. KLF14 deficiency is associated with protection from colitis, and interestingly KLF14 is also inversely associated with FOXP3 in T cells isolated from patients with Crohn's disease. KLF10 and KLF14, members of the same family and both induced by TGFβ, recruit different histone-modifying complexes and, as demonstrated in our current and previous publications, bind to different elements of the FOXP3 promoter locus.[1,2] These data suggest that the KLF network-regulating T-cell differentiation has relevance to intestinal homeostasis and colitis.

In conclusion, we previously demonstrated that KLF10 directly regulates the promoter of FOXP3 in vivo and that alteration of this process impairs Treg cellular differentiation, leading to the development of autoimmunity. As a direct extension of these studies, we now report that KLF14, a protein structurally and functionally related to KLF10, also regulates the differentiation and functional specialization of Treg cells. Our findings demonstrate, for the first time, that 1) KLF14 is highly expressed in the immune system, in particular in Treg cells, where it functions as a transcriptional repressor of the FOXP3 gene; 2) KLF14 KO mice, which carry hypersuppressive Treg cells, are protected from experimentally induced colitis; and 3) the increase in FOXP3 levels observed in KLF14 KO Treg cells involves epigenetic modifications at the TSDR, the intronic enhancer region associated with stable expression of this gene. This work furthers our knowledge into how FOXP3 is repressed and/or silenced during Treg cell differentiation and lineage determination, and/or in conditions of immunopathogenesis.

References

1. Xiong Y, Khanna S, Grzenda AL, et al. Polycomb antagonizes p300/CREB-binding protein-associated factor to silence FOXP3 in a Kruppel-like factor-dependent manner. J Biol Chem 2012;287:34372–34385.
2. Xiong Y, Svingen PA, Sarmento OO, et al. Differential coupling of KLF10 to Sin3-HDAC and PCAF regulates

the inducibility of the FOXP3 gene. Am J Physiol Regul Integr Comp Physiol 2014;307:R608–R620.
3. de Assuncao TM, Lomberk G, Cao S, et al. New role for Kruppel-like factor 14 as a transcriptional activator involved in the generation of signaling lipids. J Biol Chem 2014;289:15798–15809.
4. Delgoffe GM, Kole TP, Zheng Y, et al. The mTOR kinase differentially regulates effector and regulatory T cell lineage commitment. Immunity 2009;30:832–844.
5. Liu G, Burns S, Huang G, et al. The receptor S1P1 overrides regulatory T cell-mediated immune suppression through Akt-mTOR. Nat Immunol 2009;10:769–777.
6. Liu G, Yang K, Burns S, et al. The S1P(1)-mTOR axis directs the reciprocal differentiation of T_H1 and T_{reg} cells. Nat Immunol 2010;11:1047–1056.
7. Procaccini C, De Rosa V, Galgani M, et al. Leptin-induced mTOR activation defines a specific molecular and transcriptional signature controlling $CD4^+$ effector T cell responses. J Immunol 2012;189:2941–2953.
8. Zeng H, Yang K, Cloer C, et al. mTORC1 couples immune signals and metabolic programming to establish T_{reg}-cell function. Nature 2013;499:485–490.
9. Rahman MK, Midtling EH, Svingen PA, et al. The pathogen recognition receptor NOD2 regulates human $FOXP3^+$ T cell survival. J Immunol 2010;184:7247–7256.
10. Nelson JD, Denisenko O, Bomsztyk K. Protocol for the fast chromatin immunoprecipitation (ChIP) method. Nature Protocols 2006;1:179–185.
11. Barzaghi F, Passerini L, Bacchetta R. Immune dysregulation, polyendocrinopathy, enteropathy, X-linked syndrome: a paradigm of immunodeficiency with autoimmunity. Front Immunol 2012;3:211.
12. Okou DT, Mondal K, Faubion WA, et al. Exome sequencing identifies a novel FOXP3 mutation in a 2-generation family with inflammatory bowel disease. J Pediatr Gastroenterol Nutr 2014;58:561–568.
13. Faubion WA, De Jong YP, Molina AA, et al. Colitis is associated with thymic destruction attenuating $CD4^+25^+$ regulatory T cells in the periphery. Gastroenterology 2004;126:1759–1770.
14. Duijvestein M, Wildenberg ME, Welling MM, et al. Pretreatment with interferon-gamma enhances the therapeutic activity of mesenchymal stromal cells in animal models of colitis. Stem Cells 2011;29:1549–1558.
15. de Jong YP, Abadia-Molina AC, Satoskar AR, et al. Development of chronic colitis is dependent on the cytokine MIF. Nat Immunol 2001;2:1061–1066.
16. Ostanin DV, Bao J, Koboziev I, et al. T cell transfer model of chronic colitis: concepts, considerations, and tricks of the trade. Am J Physiol Gastrointest Liver Physiol 2009;296:G135–G146.
17. Chauhan SK, Saban DR, Lee HK, et al. Levels of Foxp3 in regulatory T cells reflect their functional status in transplantation. J Immunol 2009;182:148–153.
18. Wu W, Weigand L, Belkaid Y, et al. Immunomodulatory effects associated with a live vaccine against *Leishmania major*. Eur J Immunol 2006;36:3238–3247.
19. Powrie F, Correa-Oliveira R, Mauze S, et al. Regulatory interactions between $CD45RB_{high}$ and $CD45RB_{low}$ $CD4^+$ T cells are important for the balance between protective and pathogenic cell-mediated immunity. J Exp Med 1994;179:589–600.
20. Polansky JK, Kretschmer K, Freyer J, et al. DNA methylation controls Foxp3 gene expression. Eur J Immunol 2008;38:1654–1663.
21. Baron U, Floess S, Wieczorek G, et al. DNA demethylation in the human FOXP3 locus discriminates regulatory T cells from activated FOXP3(+) conventional T cells. Eur J Immunol 2007;37:2378–2389.
22. Chin HG, Esteve P-O, Pradhan M, et al. Automethylation of G9a and its implication in wider substrate specificity and HP1 binding. Nucleic Acids Res 2007;35:7313–7323.
23. Fuks F, Hurd PJ, Deplus R, et al. The DNA methyltransferases associate with HP1 and the SUV39H1 histone methyltransferase. Nucleic Acids Res 2003;31:2305–2312.
24. Mathison A, Grzenda A, Lomberk G, et al. Role for Krüppel-like transcription factor 11 in mesenchymal cell function and fibrosis. PLoS One 2013;8:e75311.
25. Hart GT, Wang X, Hogquist KA, et al. Kruppel-like factor 2 (KLF2) regulates B-cell reactivity, subset differentiation, and trafficking molecule expression. Proc Natl Acad Sci USA 2011;108:716–721.
26. Kwon SJ, Crespo-Barreto J, Zhang W, et al. KLF13 cooperates with c-Maf to regulate IL-4 expression in $CD4^+$ T cells. J Immunol 2014;192:5703–5709.
27. Pabbisetty SK, Rabacal W, Maseda D, et al. KLF2 is a rate-limiting transcription factor that can be targeted to enhance regulatory T-cell production. Proc Natl Acad Sci USA 2014;111:9579–9584.
28. Preston GC, Feijoo-Carnero C, Schurch N, et al. The impact of KLF2 modulation on the transcriptional program and function of CD8 T cells. PLoS One 2013;8:e77537.
29. Sebzda E, Zou Z, Lee JS, et al. Transcription factor KLF2 regulates the migration of naive T cells by restricting chemokine receptor expression patterns. Nat Immunol 2008;9:292–300.
30. Takada K, Wang X, Hart GT, et al. Kruppel-like factor 2 is required for trafficking but not quiescence in post-activated T cells. J Immunol 2011;186:775–783.
31. Weinreich MA, Takada K, Skon C, et al. KLF2 transcription-factor deficiency in T cells results in unrestrained cytokine production and upregulation of bystander chemokine receptors. Immunity 2009;31:122–130.
32. Winkelmann R, Sandrock L, Kirberg J, et al. KLF2—a negative regulator of pre-B cell clonal expansion and B cell activation. PLoS One 2014;9:e97953.
33. Winkelmann R, Sandrock L, Porstner M, et al. B cell homeostasis and plasma cell homing controlled by Kruppel-like factor 2. Proc Natl Acad Sci USA 2011;108:710–715.
34. Cao Z, Wara AK, Icli B, et al. Kruppel-like factor KLF10 targets transforming growth factor-beta1 to regulate $CD4^+CD25^-$ T cells and T regulatory cells. J Biol Chem 2009;284:24914–24924.
35. Lai D, Zhu J, Wang T, et al. KLF13 sustains thymic memory-like $CD8^+$ T cells in BALB/c mice by regulating IL-4-generating invariant natural killer T cells. J Exp Med 2011;208:1093–1103.

36. Iwasa T, Nakamura K, Ogino H, et al. Multiple ulcers in the small and large intestines occurred during tocilizumab therapy for rheumatoid arthritis. Endoscopy 2011; 43:70–72.
37. Wildin RS, Ramsdell F, Peake J, et al. X-linked neonatal diabetes mellitus, enteropathy and endocrinopathy syndrome is the human equivalent of mouse scurfy. Nat Genet 2001;27:18–20.
38. Bennett CL, Christie J, Ramsdell F, et al. The immune dysregulation, polyendocrinopathy, enteropathy, X-linked syndrome (IPEX) is caused by mutations of FOXP3. Nat Genet 2001;27:20–21.
39. Wildin RS, Smyk-Pearson S, Filipovich AH. Clinical and molecular features of the immunodysregulation, polyendocrinopathy, enteropathy, X linked (IPEX) syndrome. J Med Genet 2002;39:537–545.
40. Humblet-Baron S, Sather B, Anover S, et al. Wiskott-Aldrich syndrome protein is required for regulatory T cell homeostasis. J Clin Invest 2007;117:407–418.
41. Gomez-Rodriguez J, Wohlfert EA, Handon R, et al. Itk-mediated integration of T cell receptor and cytokine signaling regulates the balance between Th17 and regulatory T cells. J Exp Med 2014;211:529–543.
42. Fragale A, Gabriele L, Stellacci E, et al. IFN regulatory factor-1 negatively regulates $CD4^+$ $CD25^+$ regulatory T cell differentiation by repressing Foxp3 expression. J Immunol 2008;181:1673–1682.
43. Floess S, Freyer J, Siewert C, et al. Epigenetic control of the foxp3 locus in regulatory T cells. PLoS Biol 2007; 5:e38.
44. Schreiber L, Pietzsch B, Floess S, et al. The Treg-specific demethylated region stabilizes *Foxp3* expression independently of NF-κB signaling. PLoS One 2014;9:e88318.
45. Polansky JK, Schreiber L, Thelemann C, et al. Methylation matters: binding of Ets-1 to the demethylated Foxp3 gene contributes to the stabilization of Foxp3 expression in regulatory T cells. J Mol Med 2010; 88:1029–1040.
46. Liu Z, Zhang C, Sun J. Deacetylase inhibitor trichostatin A down-regulates Foxp3 expression and reduces $CD4^+CD25^+$ regulatory T cells. Biochem Biophys Res Comm 2010;400:409–412.
47. Antignano F, Burrows K, Hughes MR, et al. Methyltransferase G9A regulates T cell differentiation during murine intestinal inflammation. J Clin Invest 2014; 124:1945–1955.
48. Graler MH, Huang MC, Watson S, et al. Immunological effects of transgenic constitutive expression of the type 1 sphingosine 1-phosphate receptor by mouse lymphocytes. J Immunol 2005;174:1997–2003.
49. Matloubian M, Lo CG, Cinamon G, et al. Lymphocyte egress from thymus and peripheral lymphoid organs is dependent on S1P receptor 1. Nature 2004;427: 355–360.
50. Shiow LR, Rosen DB, Brdickova N, et al. CD69 acts downstream of interferon-alpha/beta to inhibit S1P1 and lymphocyte egress from lymphoid organs. Nature 2006; 440:540–544.

Received July 18, 2014. Accepted December 12, 2014.

Correspondence
Address correspondence to: William A. Faubion, MD, 200 First Street SW, Rochester, Minnesota 55905. e-mail: faubion.william@mayo.edu; fax: (507) 255-6318.

Conflicts of interest
The authors disclose no conflicts.

Funding
This study was funded by a Research Fellows Award from the Crohn's & Colitis Foundation of America (Award Number: 271332), and grants from the National Institute of Allergy and Infectious Diseases, and the Leona Helmsley Charitable Trust Foundation (to W.A.F.) (NIH NIAID AI89714-R01) and NIDDK52913, P30-DK084567, and NCI CA178627 (to R.U.).

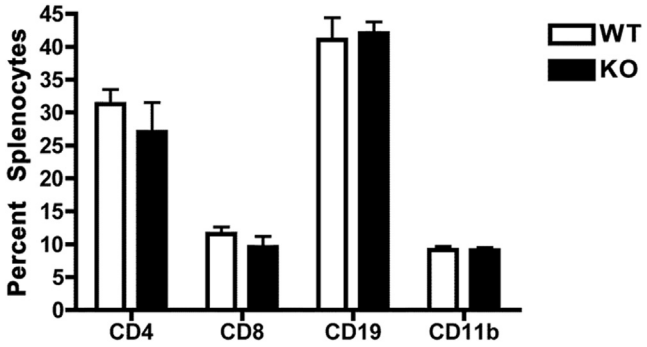

Supplementary Figure 1. KLF14 KO mice demonstrate normal CD4:CD8 ratio and normal populations of CD19$^+$ and CD11b$^+$ cells within the spleen when compared to age- and sex-matched control mice. The histogram represents results from flow cytometric analysis of splenocytes for CD4, CD8, B cell (CD19), and myeloid (CD11b) lineage cells. Note no demonstrable differences in above subsets (WT *open histogram*, KLF14 KO *closed histogram*). The data represent the mean/standard error of the mean of three independent experiments. A nonparametric, unpaired *t* test of significance between lymphoid organs (Mann-Whitney) demonstrated no statistically significant difference.

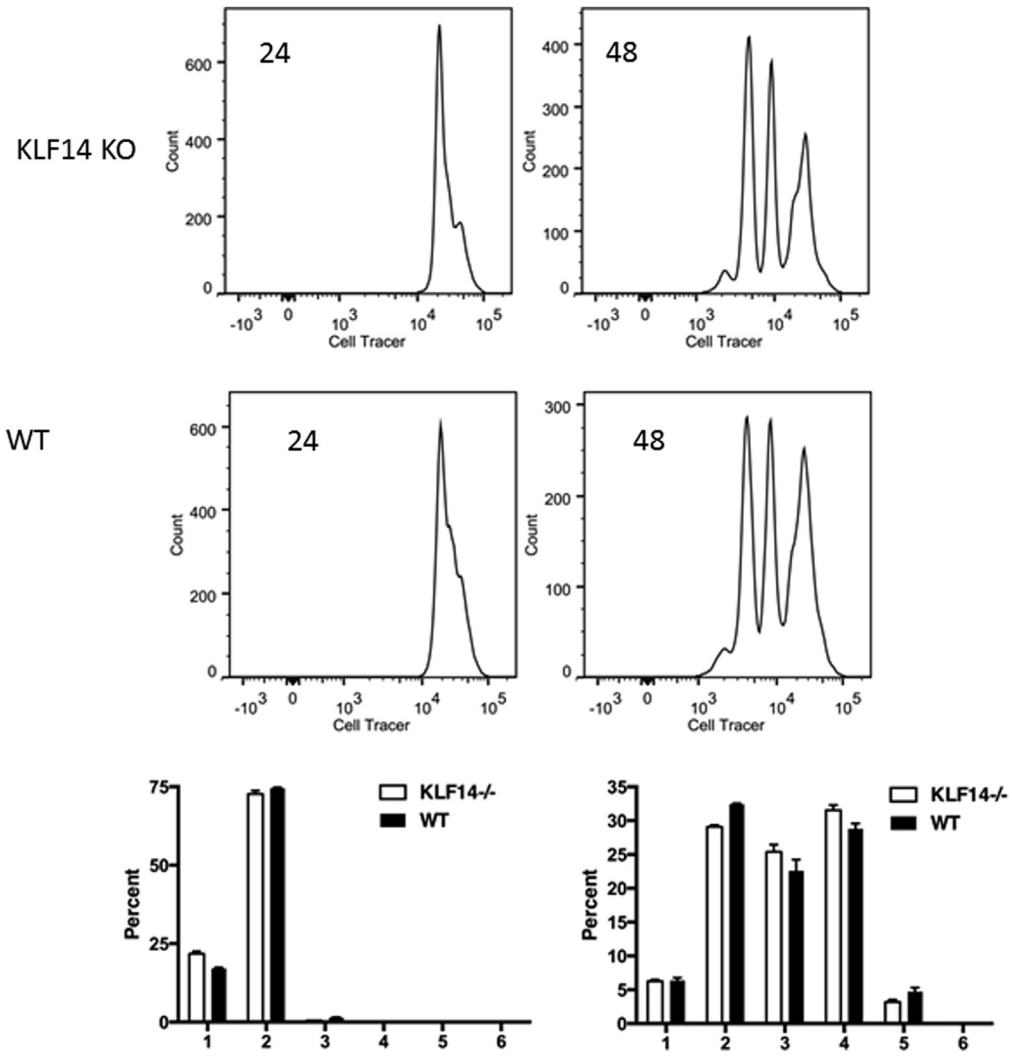

Supplementary Figure 2. KLF14 KO CD4$^+$ T cells demonstrate normal kinetics of proliferation. Histograms represent fluorescent intensity of CellTrace Violet in naïve KLF14 KO (*upper panels*) and WT (*second row*) CD4$^+$ T cells after stimulation with TCR and TGFβ for 24 (*left column*) or 48 hours of stimulation. Note the similar profiles of fluorescent dilution with subsequent cell proliferative cycles between KLF14 KO versus WT. Quantitation of lymphocytes present in flow cytometric gates in triplicate experiments is presented in histograms below. Note no significant differences between KLF14 KO (*open histogram*) and WT (*closed histogram*) cells represented within each cell division. The experiment was performed in triplicate and histograms represent mean/standard error of the mean of all data. Multiple *t* test analysis was performed using the Holm-Sidak method, with alpha = 5.000% ($P < .05$). Each time point was analyzed individually, without assuming a consistent standard deviation. No statistically significant difference between genotypes was evident.

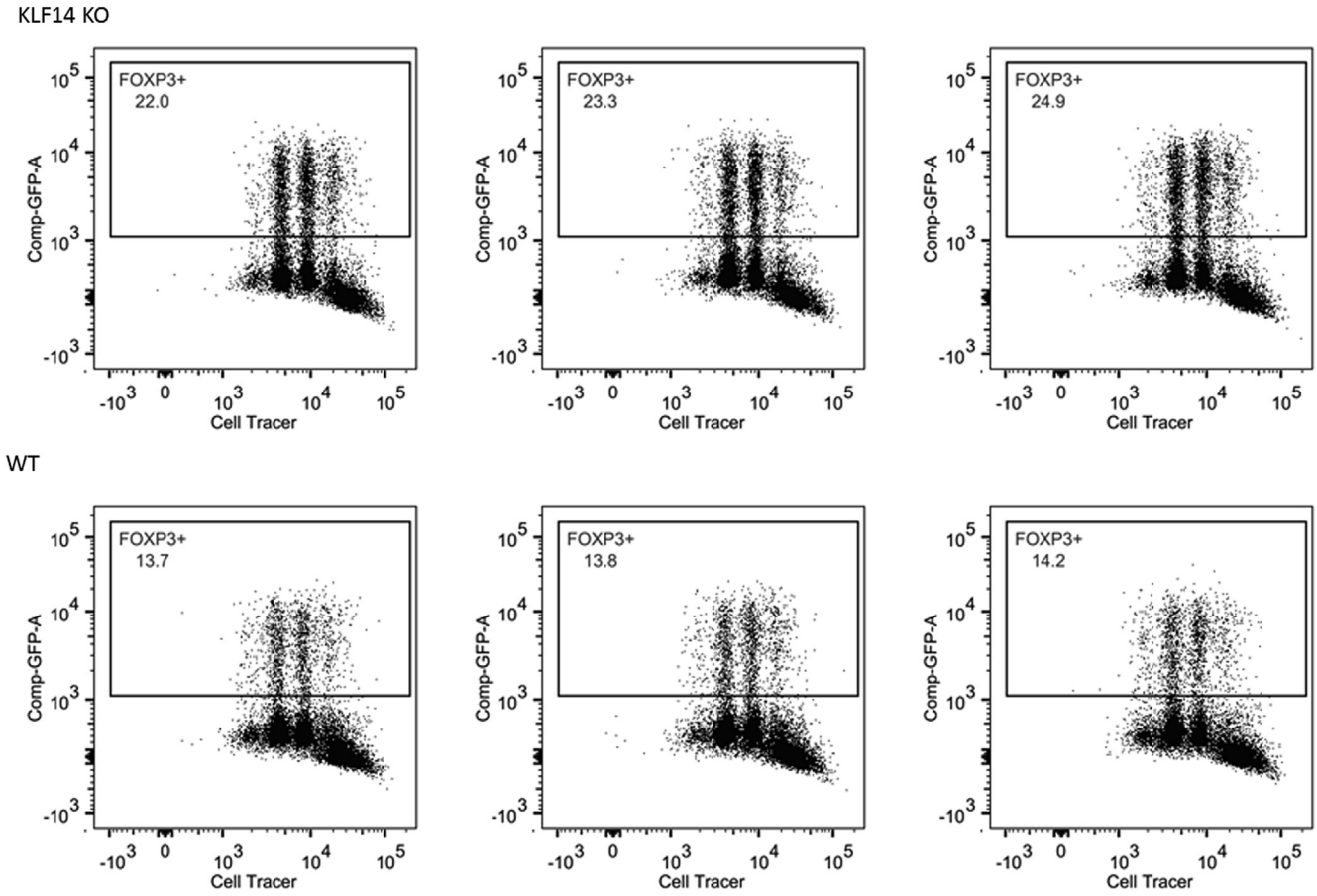

Supplementary Figure 3. KLF14 KO CD4$^+$ FOXP3$^+$ T cells demonstrate normal kinetics of proliferation. Dot plots represent fluorescent intensity of CellTrace Violet in naïve KLF14 KO (*upper panels*) and WT (*lower panels*) CD4$^+$ T cells after stimulation with TCR and TGFβ for 24 (*left column*), 48 (*middle column*), or 72 (*right column*) hours of stimulation. FOXP3$^+$ cells are GFP$^+$ cells on the *y* axis, and the box represents FOXP3$^+$ cells expressed as a percentage of CD4$^+$ cells. Note the similar profiles of fluorescent dilution with subsequent cell proliferative cycles between KLF14 KO versus WT FOXP3$^+$ cells and, as observed previously, the higher percentage of FOXP3$^+$ cells in the KLF14 KO cells. The experiment was performed in triplicate, and all data are shown.

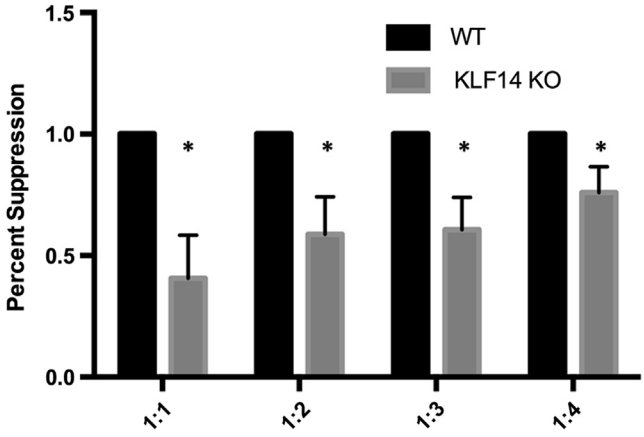

Supplementary Figure 4. KLF14-deficient T-regulatory (Treg) cells demonstrate enhanced suppression in vitro. Histogram represents thymidine incorporation of T responder cells (WT) in coculture with Treg cells isolated from WT (*black column*) or KLF14 KO mice (*grey column*) normalized to WT. 1:1 = 60% reduction, $P = .0002$; 1:2 = 41% reduction, $P = .002$; 1:3 = 40% reduction, $P = .004$; 1:4 = 24% reduction, $P = .03$. Presented are the mean and standard deviation (SD) of thymidine counts conducted in triplicate. Data are representative of three independent experiments. Statistical significance was determined using the Holm-Sidak method, with alpha = 5.000% ($P < .05$). Each titration was analyzed individually, without assuming a consistent SD.

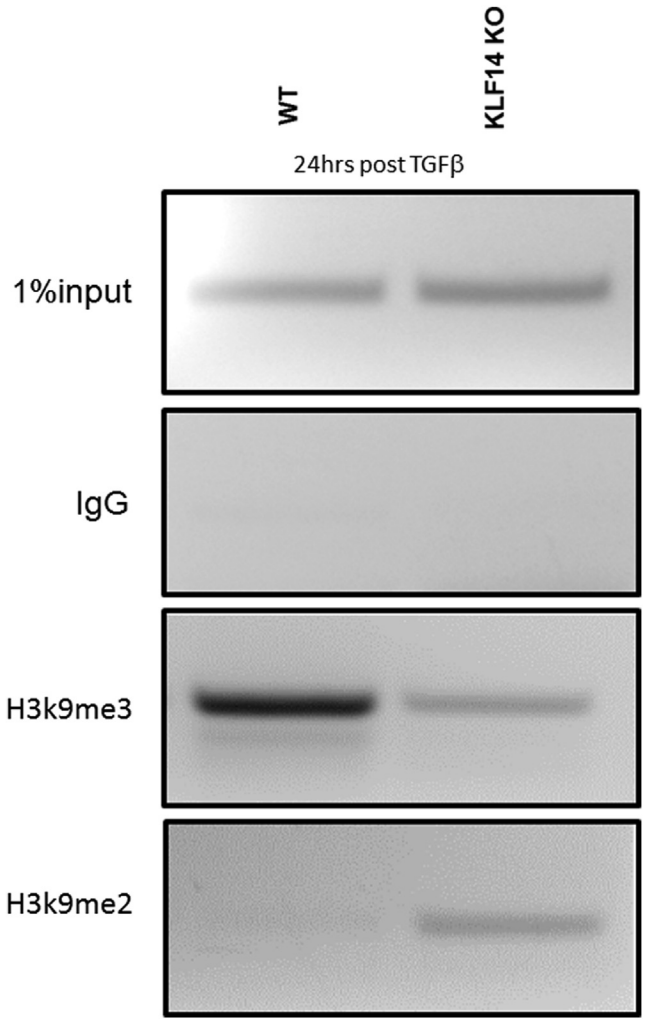

Supplementary Figure 5. KLF14 KO associates with H3K9me2 histone marks at the TSDR. Semiquantitative PCR ChIP analysis of the expression of FOXP3 in cell fractions after immunoprecipitation for H3K9me2 shows higher levels of the modification in KLF14 KO naïve cells stimulated in T regulatory (Treg) conditions for 24 hours in comparison with WT cells, inverse to the H3K9me3 mark. Data are representative of three independent experiments.